SUMOylation of DNA topoisomerase IIα regulates histone H3 kinase Haspin and H3 phosphorylation in mitosis

Makoto M. Yoshida,[1] Lily Ting,[2] Steven P. Gygi,[2] and Yoshiaki Azuma[1]

[1]Department of Molecular Biosciences, University of Kansas, Lawrence, KS 66045
[2]Department of Cell Biology, Harvard Medical School, Boston, MA 02115

DNA topoisomerase II (TOP2) plays a pivotal role in faithful chromosome separation through its strand-passaging activity that resolves tangled genomic DNA during mitosis. Additionally, TOP2 controls progression of mitosis by activating cell cycle checkpoints. Recent work showed that the enzymatically inert C-terminal domain (CTD) of TOP2 and its post-translational modification are critical to this checkpoint regulation. However, the molecular mechanism has not yet been determined. By using *Xenopus laevis* egg extract, we found that SUMOylation of DNA topoisomerase IIα (TOP2A) CTD regulates the localization of the histone H3 kinase Haspin and phosphorylation of histone H3 at threonine 3 at the centromere, two steps known to be involved in the recruitment of the chromosomal passenger complex (CPC) to kinetochores in mitosis. Robust centromeric Haspin localization requires SUMOylated TOP2A CTD binding activity through SUMO-interaction motifs and the phosphorylation of Haspin. We propose a novel mechanism through which the TOP2 CTD regulates the CPC via direct interaction with Haspin at mitotic centromeres.

Introduction

Cell stage–specific kinases are important for the progression of mitosis. These kinases play a role in specific pathways to ensure that chromosomes segregate properly to daughter cells to prevent aneuploidy. Among the mitotic kinases, Aurora B plays a central role in the maintenance of genome stability by activating the spindle assembly checkpoint in response to improper kinetochore–microtubule attachment and tension during early mitosis (Lan et al., 2004; Cheeseman et al., 2006; Cimini et al., 2006; DeLuca et al., 2006; Pinsky et al., 2006; Welburn et al., 2010). Aurora B kinase localizes at the centromere during early mitosis, and its centromeric localization is achieved by its interaction with other members of the chromosomal passenger complex (CPC): INCENP, Borealin, and Survivin (Adams et al., 2000; Kaitna et al., 2000; Gassmann et al., 2004). Several mechanisms for CPC recruitment at mitotic centromeres exist in eukaryotes (Carmena et al., 2012). Among them, two mechanisms rely on the mitosis-specific phosphorylation of histone tails. Bub1-dependent phosphorylation of H2A threonine 120 (serine 121 in fission yeast) allows for its interaction with Shugoshin proteins, which can then interact and recruit the CPC by binding with Borealin (Kawashima et al., 2010; Yamagishi et al., 2010). The other mechanism is the recruitment of CPC to the centromere through the activity of histone H3 kinase Haspin, which phosphorylates histone H3 at threonine 3 (H3T3) for its direct interaction with the BIR domain of Survivin (Kelly et al., 2010; Jeyaprakash et al., 2011). A previous study suggested that the cohesin-associated factor Pds5 may help target Haspin to chromosomes in fission yeast (Yamagishi et al., 2010). However, the mechanism of how Haspin localizes onto the chromosomes to target centromeric histone H3 in vertebrates remains unclear. CPC recruitment at mitotic centromeres uses multiple molecular mechanisms, suggesting that different signals can control specific pathways.

DNA topoisomerase II (TOP2) has a critical role during mitosis for resolving tangled genomic DNA by its strand-passaging enzymatic reaction (Holm et al., 1985). Inhibition of TOP2 activity could activate cell cycle checkpoints, including the DNA damage checkpoint, because of double-stranded breaks mediated by TOP2 (Nitiss, 2009). A proposed mechanism of TOP2-initiated G2 arrest is the binding of MDC1 to the phosphorylated TOP2 C-terminal domain (Luo et al., 2009). More recently, Furniss et al. (2013) showed that specific mutations of TOP2 that alter its strand-passaging reaction at specific steps could induce a Mad2-dependent delay in mitosis in budding yeast. Interestingly, this checkpoint activation requires the C-terminal domain (CTD) of TOP2, which suggests that TOP2

Correspondence to Yoshiaki Azuma: azumay@ku.edu

Abbreviations used in this paper: CPC, chromosomal passenger complex; CSF, cytostatic factor; CTD, C-terminal domain; dnUbc9, dominant-negative Ubc9; H3T3p, phosphorylated histone H3 threonine 3; LC-MS/MS, liquid chromatography–tandem mass spectrometry; SENP2 CD, sentrin-specific protease 2 catalytic domain; SIM, SUMO-interacting motif; TOP2, DNA topoisomerase II; WT, wild type; XEE, *X. laevis* egg extract.

The Rockefeller University Press $30.00
J. Cell Biol. Vol. 213 No. 6 665–678
www.jcb.org/cgi/doi/10.1083/jcb.201511079

CTD has a critical role in controlling cell cycle progression, and the domain could serve as a signal transducer for cell cycle checkpoints. Notably, TOP2 has been reported to be involved in Aurora B activation, suggesting that TOP2 can control mitotic checkpoints via Aurora B (Coelho et al., 2008).

Although TOP2 could be modified with both SUMO1 and SUMO2/3, topoisomerase IIα (TOP2A) has been reported to be modified primarily by SUMO2/3 during mitosis in *Xenopus laevis* (Mao et al., 2000; Azuma et al., 2003; Agostinho et al., 2008). Recently, we have shown that SUMOylation of TOP2A CTD facilitates novel interaction with DNA damage checkpoint adaptor protein Claspin in *X. laevis* egg extracts (XEEs; Ryu et al., 2015). Claspin binds to Chk1, a kinase known to activate Aurora B by phosphorylating serine 311 in human cells (Kumagai and Dunphy, 2000; Petsalaki et al., 2011). Therefore, SUMOylated TOP2A could be involved in Aurora B activation by Chk1 recruitment via Claspin. In addition to the potential Aurora B regulation by Claspin, we have identified Haspin as a binding protein of SUMOylated CTD by comprehensive liquid chromatography–tandem mass spectrometry (LC-MS/MS) analysis. Both Haspin and phosphorylated H3T3 (H3T3p) were less abundant on mitotic chromosomes when TOP2A SUMOylation was prevented. Robust binding of Haspin to SUMOylated TOP2A required Haspin's SUMO-interacting motifs (SIMs) and the phosphorylation of Haspin, and mutations in both T206 and SIMs prevented Haspin from properly localizing at mitotic centromeres. Altogether, our results show that SUMOylated TOP2A regulates the targeting of active Haspin to mitotic centromeres for the phosphorylation of H3T3. We propose that this novel mechanism of Haspin recruitment mediated by SUMOylated TOP2A CTD may be another molecular mechanism that regulates the progression of mitosis by regulating Aurora B at mitotic centromeres.

Results

SUMOylation contributes to the localization of Aurora B kinase on mitotic chromosomes

SUMOylation has previously been reported to be essential for proper chromosome segregation during mitosis (Tanaka et al., 1999; Biggins et al., 2001; Bachant et al., 2002; Azuma et al., 2003). We recently identified Claspin as a SUMOylated TOP2A-binding protein and demonstrated that inhibition of mitotic SUMOylation resulted in defective centromeric localization of Claspin, which is known to bind to Chk1 (Kumagai and Dunphy, 2000; Ryu et al., 2015). Because Chk1 can activate Aurora B, our finding led us to investigate whether Aurora B was affected by the SUMOylation occurring on the mitotic chromosomes (Petsalaki et al., 2011). We inhibited mitotic SUMOylation specifically through the addition of dominant-negative mutant E2 enzyme Ubc9 (dnUbc9) in XEEs after the completion of DNA replication and before the onset of mitotic induction (Fig. 1 A). Immunoblotting analysis of Aurora B on replicated mitotic chromosomes indicated that the inhibition of mitotic SUMOylation reduced levels of both Aurora B and autophosphorylated Aurora B T248 (T232 in humans) on the mitotic chromosomes (Fig. 1 B). Aurora B levels were reduced by 20%, whereas phosphorylated and activated Aurora B levels were reduced by 35% on the mitotic chromosomes with the addition of dnUbc9 (Fig. 1 C). Furthermore, immunofluorescence staining of the mitotic chromosomes showed that the inhibition of SUMOylation reduced Aurora B localization at the centromeres (Fig. 1 D). Consistent with the immunoblotting results, the immunofluorescence signal intensity of Aurora B at the centromere was significantly reduced, by 34% (Fig. 1 E). These results suggest that mitotic SUMOylation could regulate centromeric Aurora B localization as well as the amount of activated Aurora B on the mitotic chromosomes.

SUMOylated DNA topoisomerase IIα interacts with Haspin through Haspin SIMs

Although SUMOylation-dependent centromeric localization of Claspin could regulate the activation of Aurora B (represented by autophosphorylated T248) via Chk1, that may not explain the reduced binding of Aurora B through the inhibition of SUMOylation on *X. laevis* mitotic chromosomes because loss of Chk1 activity did not alter Aurora B localization in human cells (Petsalaki et al., 2011). Therefore, mitotic SUMOylation may regulate an additional mechanism for the robust binding of Aurora B to mitotic centromeres. To determine a connection between SUMOylated TOP2A and Aurora B, we looked to identify SUMOylated TOP2A CTD-binding proteins. For the comprehensive identification of SUMOylated TOP2A CTD-binding proteins, recombinant *X. laevis* TOP2A CTD modified with SUMO2 by in vitro SUMOylation assay was prepared, as previously reported, to be used to pull down proteins from XEEs through pull-down assays (Ryu et al., 2015). Pulled-down proteins on the beads were eluted with urea after being digested by SUMO protease SENP2 (Fig. 2 A). SENP2 cleaves the conjugated SUMO2 protein from the modified TOP2A CTD, which allows for the pulled-down proteins to dissociate from the TOP2A CTD-bound beads and eliminates the high-molecular-weight contaminants of SUMOylated CTD bands in the samples. Urea-eluted proteins from both non-SUMOylated TOP2A CTD and TOP2A CTD SUMOylated with SUMO2 (CTD-SUMO) were subjected to LC-MS/MS analysis. LC-MS/MS identified multiple peptides of 61 proteins that were pulled down with CTD-SUMO but not with the non-SUMOylated CTD (Table S1). Proteins identified included known SUMO-interacting proteins SETDB1 and RNF4 (Häkli et al., 2005; Rosendorff et al., 2006). Among the identified candidate proteins that were pulled down with CTD-SUMO and that could regulate Aurora B was histone H3 kinase Haspin. Immunoblotting analysis of the pull-down samples confirmed that Haspin bound specifically to the SUMOylated form of TOP2A CTD (Fig. 2 B). Therefore, Haspin was a potential target that could mediate Aurora B binding on the mitotic chromosomes in a SUMOylation-dependent manner. Haspin was previously reported to interact with Pds5, and the deletion of Pds5 could cause a reduction in H3T3 phosphorylation and the centromeric localization of Aurora B (Yamagishi et al., 2010; Carretero et al., 2013). However, neither *X. laevis* Pds5a nor Pds5b was pulled down with either CTD or CTD-SUMO, suggesting that Pds5 is not involved in the protein interaction between SUMOylated TOP2A CTD and Haspin (Fig. S1).

Because a SUMO-interacting motif (SIM), a short sequence of large hydrophobic residues, can allow proteins to directly interact with SUMO on SUMOylated proteins (Song et al., 2004, 2005; Hecker et al., 2006; Ryu et al., 2015), we analyzed Haspin's primary sequence using a SIM prediction program to determine whether Haspin possessed any SIMs (Xue et al., 2006). We identified two potential SIMs near the

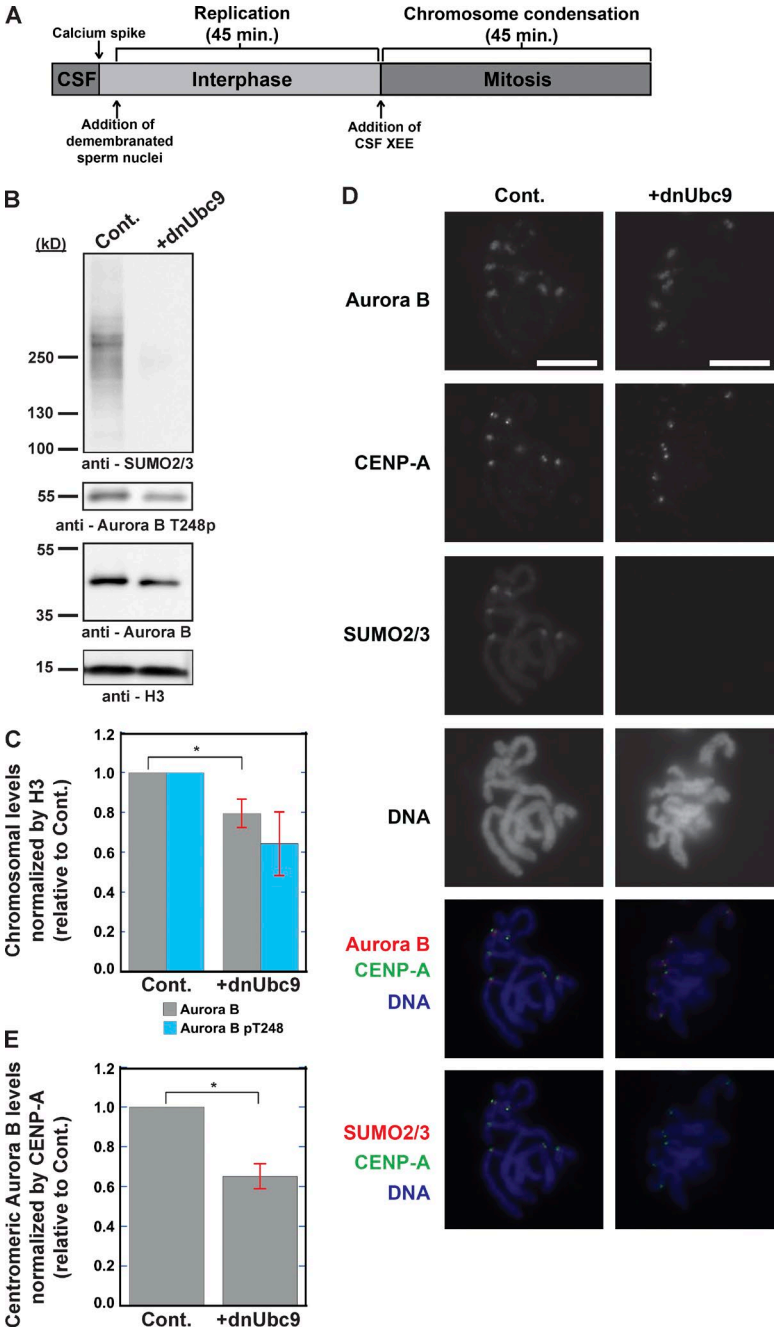

Figure 1. **Inhibition of SUMOylation reduces Aurora B kinase on mitotic chromosomes.** (A) Schematic method for the preparation of mitotic replicated chromosomes from XEEs. (B) Mitotic replicated chromosomes isolated as in A with (+dnUbc9) or without (control [Cont.]) dnUbc9 were subjected to immunoblotting. Histone H3 was used for the loading control for the mitotic chromosomes. (C) Quantification of Aurora B and Aurora B T248p levels on the mitotic chromosome, as seen in B, relative to levels of Cont. chromosomes from three independent experiments (n = 3) with levels normalized to histone H3 levels. Error bars represent SD. *, $P < 0.05$ (Student's t test). (D) Mitotic replicated chromosomes prepared as in A with or without dnUbc9 (Cont.) were subjected to immunofluorescence staining with antibodies as indicated with Hoechst 33342. Bar, 10 µm. (E) Quantification of the Aurora B signal intensity at mitotic centromeres, as seen in D, relative to signal intensities of Cont. centromeres from three independent experiments (n = 3, 50 centromeres per n) with levels normalized to CENP-A signal. Error bars represent SD. *, $P < 0.05$ (Student's t test).

N-terminal region of Haspin at aa 343–346 (VICL) and 364–367 (VLCL; Fig. 2 C). To determine whether these sequences were important for Haspin's interaction with SUMOylated TOP2A, we created a double SIM mutant (2-SIM) Haspin construct in pTGFC70 with a GFP-tag and a 3′ UTR of xKid (Ghenoiu et al., 2013). Using mRNA created from the construct, we expressed either the wild-type (WT) Haspin-GFP or Haspin-GFP 2-SIM in XEEs separately at similar levels, and the Haspin-GFP–expressing XEEs arrested in metaphase with cytostatic factor (CSF XEEs) were subjected to pull-down assays with CTD-SUMO (Fig. 2 D). Immunoblotting analysis showed that the expressed Haspin 2-SIM bound 48% less to CTD-SUMO than Haspin WT (Fig. 2 E). This indicates that the SIMs contribute to the robust binding of Haspin to SUMOylated TOP2A CTD. However, although mutations in the SIMs reduced the binding of Haspin to CTD-SUMO, they did not completely eliminate its binding capability, which suggests that another factor may be involved in the interaction.

Haspin localizes at mitotic centromeres for H3T3 phosphorylation in a SUMOylation-dependent manner

Because TOP2A SUMOylation occurs primarily at the centromere during mitosis (Azuma et al., 2005; Ryu and Azuma, 2010; Ryu et al., 2010b) and can regulate the centromeric localization of Claspin as previously reported, we hypothesized that the localization of Haspin is dependent on the SUMOylation occurring on the mitotic chromosomes. To address this, we first examined whether mitotic SUMOylation in XEEs can regulate the binding of Haspin on the chromosomes. When SUMO

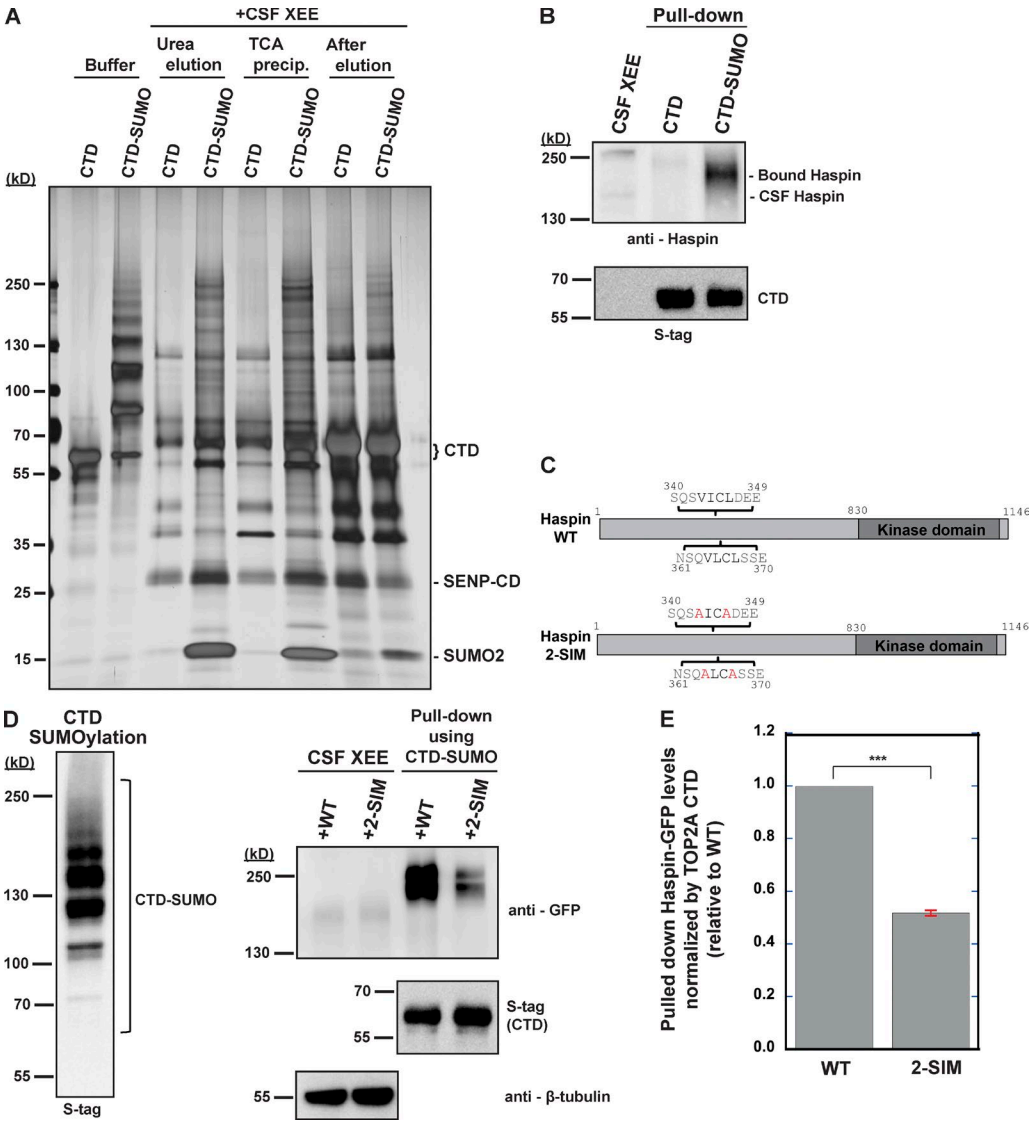

Figure 2. **Haspin binding to TOP2A CTD is dependent on SUMOylation and SIMs.** (A) Silver stain of the pulled-down proteins using TOP2A CTD. S-tagged non-SUMOylated (CTD) and SUMOylated CTD (CTD-SUMO) through in vitro SUMOylation assay were bound to S-agarose beads and incubated with CSF XEEs for pull-down assay. After incubation with SENP2 CD, proteins were eluted with urea and precipitated with trichloroacetic acid (TCA precip.). Lanes 1 and 2 represent 5% of the S-tagged CTD and CTD-SUMO bound onto S-agarose beads as bait. Proteins in each fraction were visualized with silver stain. After elution, samples were the proteins remaining on S-agarose beads. Trichloroacetic acid–precipitated fractions were subjected to protein identification by LC-MS/MS. (B) SENP2-digested pull-down samples were analyzed by immunoblotting for Haspin. SENP2-digested S-tagged CTD was used as a loading control for the bait used in the pull-down assay. CSF lane represents 0.75% of the volume of XEEs used for each pull-down sample. CSF Haspin indicates the endogenous band found in the CSF XEEs, and Bound Haspin indicates the Haspin band in the pull-down sample. (C) Schematic representation of the primary structure of *X. laevis* Haspin. SIMs are located at aa 343–346 (VICL) and 364–367 (VLCL). Point mutations in each SIM are indicated in red for the disrupted SIM mutant protein (2-SIM). (D) mRNAs of GFP-tagged WT or 2-SIM Haspin were supplemented in XEEs to express Haspin-GFP, and Haspin-GFP–expressing CSF XEEs were subjected to the pull-down assay with S-tagged CTD SUMOylated (CTD-SUMO) through in vitro SUMOylation assay and bound onto S-agarose beads (middle). After SENP2-CD incubation, CTD-SUMO–bound Haspin-GFP was analyzed by immunoblotting (right). SENP2-digested S-tagged CTD was used as a loading control for the bait used in the pull-down assay. CSF XEE lanes represent 0.5% of the volume of the Haspin-GFP–expressing CSF XEEs used for each pull-down sample. (E) Quantification of pulled-down Haspin-GFP levels by CTD-SUMO, as seen in D, relative to Haspin-GFP WT levels from three independent experiments ($n = 3$) with levels normalized by CTD levels. Error bar represents SD. ***, $P < 0.001$ (Student's *t* test).

modification was present on mitotic chromosomes, Haspin bound to mitotic chromosomes prominently (Fig. 3 A). However, inhibiting SUMOylation with the addition of dnUbc9 reduced the levels of Haspin bound on the mitotic chromosomes by 50% (Fig. 3 B). Also, H3T3p was reduced by 22% on the SUMOylation-inhibited mitotic chromosomes. These results suggest that the reduction in Haspin on the chromosomes without SUMOylation occurring may reduce activity of Haspin on the chromosomes. Immunofluorescence staining of H3T3p on the mitotic chromosomes showed that inhibiting SUMOylation reduced its centromeric signal by 31% (Fig. 3, C and D; and Fig. S2). To determine whether the localization of Haspin on the mitotic chromosomes is affected by the inhibition of SUMOylation, we expressed Haspin-GFP in XEEs with the addition of Haspin-GFP mRNA. The colocalization of Haspin-GFP with centromeric SUMO2/3 and CENP-A (Fig. 4 A) indicated that Haspin localizes at the centromere to phosphorylate H3T3, as suggested by previous studies (Dai et al., 2005; Wang

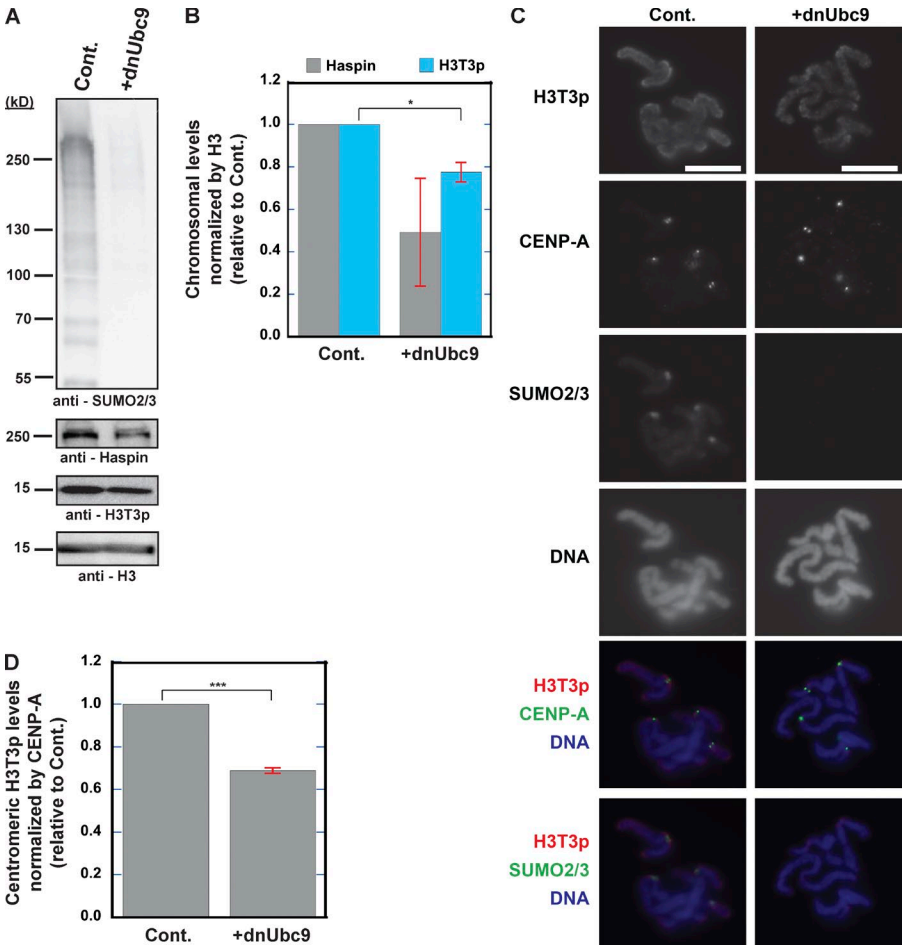

Figure 3. **SUMOylation on mitotic chromosomes regulates Haspin binding and H3T3 phosphorylation.** (A) Mitotic replicated chromosomes prepared as in Fig. 1 A with (Cont.) or without (+dnUbc9) mitotic SUMOylation. Isolated chromosomes were analyzed by immunoblotting with indicated antibodies. Histone H3 was used as a loading control for the mitotic replicated chromosomes. (B) Quantification of Haspin and H3T3p levels on the mitotic replicated chromosomes, as seen in A, relative to levels of Cont. chromosomes from three independent experiments (n = 3) with levels normalized to histone H3 levels. Error bar represents SD. *, $P < 0.05$ (Student's t test). (C) Mitotic replicated chromosomes prepared from CSF XEEs with (Cont.) or without (+dnUbc9) mitotic SUMOylation were subjected to immunofluorescence staining with antibodies as indicated with Hoechst 33342. (D) Quantification of H3T3p signal intensity at the mitotic centromeres, as seen in C, relative to signal intensities of Cont. centromeres from three independent experiments (n = 3, 40 centromeres per n) with levels normalized to CENP-A. Error bar represents SD. ***, $P < 0.001$ (Student's t test).

et al., 2010). However, the inhibition of SUMOylation caused a reduction of Haspin-GFP at mitotic centromeres, with signal intensity 21% of that when SUMOylation was present (Fig. 4 B). From these results, we conclude that mitotic SUMOylation contributes to the centromeric Haspin localization as well as the phosphorylation of centromeric H3T3. Interestingly, whereas exogenous Haspin-GFP expression also showed the localization of Haspin on the chromosomal arm regions, the inhibition of SUMOylation reduced those signals as well.

TOP2A C-terminal SUMOylation regulates Haspin binding and H3T3 phosphorylation on mitotic chromosomes

Although inhibition of mitotic SUMOylation reduced the binding of Haspin and H3T3p levels on the chromosomes, dnUbc9 addition inhibited not only the SUMOylation of TOP2A in XEEs, but other proteins that are known to be SUMOylated at the mitotic centromeres as well (Ryu et al., 2010a; Sridharan et al., 2015). To address whether SUMOylation of TOP2A CTD is responsible for the regulation of Haspin, we prepared mitotic chromosomes using recombinant TOP2A WT or 3KR (in which all three known SUMO acceptor lysines on the CTD were mutated to arginine; Ryu et al., 2015) by removing endogenous TOP2A from the XEEs through immunodepletion while adding back the recombinant TOP2A (Fig. 5, A and B). Chromosomes were assembled in TOP2A-replaced CSF XEEs, and Haspin and H3T3p levels were analyzed on the chromosomes by immunoblotting. When endogenous TOP2A was replaced by recombinant TOP2A WT, endogenous Haspin and H3T3p on the mitotic chromosomes were reduced by 39% and 36%, respectively, in the presence of dnUbc9 (Fig. 5, B and C). However, mitotic chromosomes from TOP2A 3KR–replaced XEEs also showed reduction of both Haspin and H3T3p, with levels reduced by 68% and 36%, respectively. Chromosomes with TOP2A 3KR with dnUbc9 present showed slightly further reduction, with Haspin levels reduced by 76% and H3T3p levels reduced by 56%, but the difference was not statistically significant compared with levels without dnUbc9. These results suggest that SUMOylation of TOP2A CTD substantially contributes to binding of Haspin on mitotic chromosomes and that the binding of Haspin is critical for the prominent phosphorylation of H3T3. Interestingly, the TOP2A 3KR–replaced XEEs with the addition of dnUbc9 revealed further reduction of both Haspin and H3T3p, which suggests that dnUbc9 addition may affect an additional recruitment mechanism of Haspin on the chromosomes other than through the SUMOylation of the C-terminal region of TOP2A.

Mitosis-specific phosphorylation of Haspin T206 regulates binding to SUMOylated TOP2A CTD

Although mutating the two SIMs reduced Haspin 2-SIM levels bound to SUMOylated TOP2A CTD through pull-down assays, it did not completely eliminate the interaction (Fig. 2, D and E). This result suggests that whereas the SUMOylation of TOP2A CTD is essential for the binding of Haspin, another factor contributes to the robust binding between SUMOylated TOP2A and Haspin. Interestingly, the molecular weight of Haspin-GFP

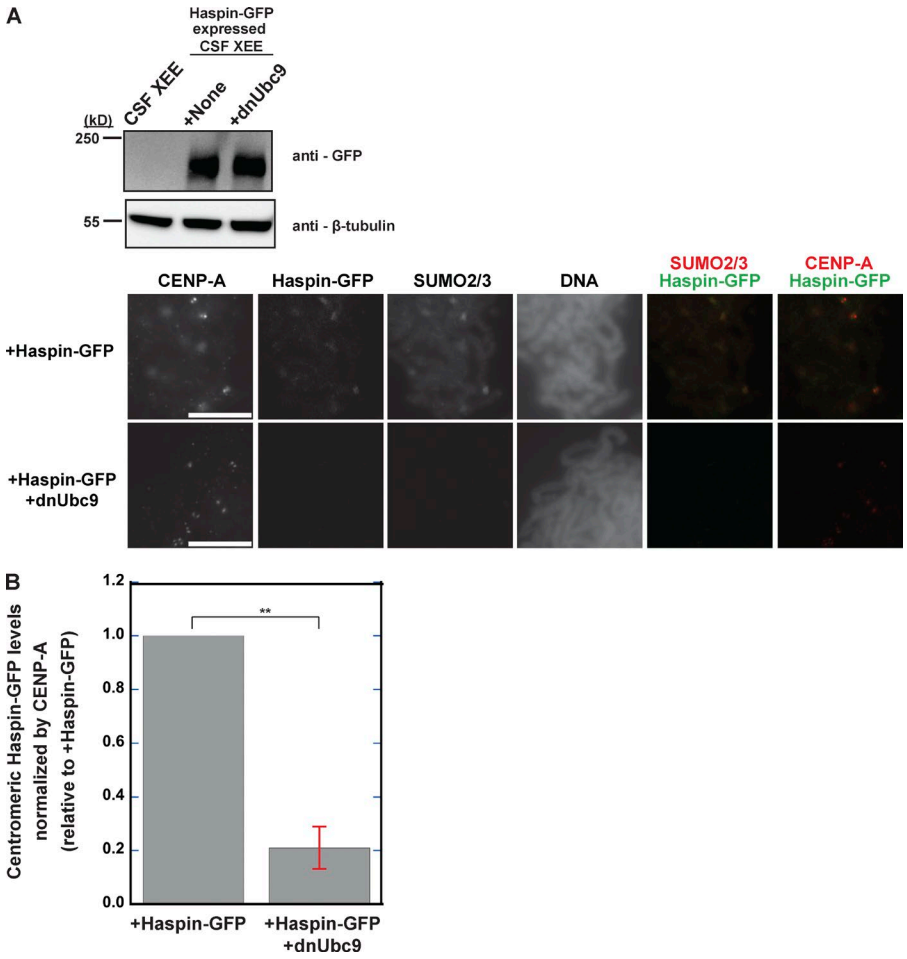

Figure 4. **SUMOylation regulates centromeric Haspin localization during mitosis.** (A) Haspin-GFP mRNA was supplemented in XEEs for protein expression (top), and mitotic replicated chromosomes prepared without or with dnUbc9 were subjected to immunofluorescence staining with indicated antibodies with Hoechst 33342. β-Tubulin was used as a loading control for Haspin-GFP expression levels in XEEs. Bar, 10 µm. (B) Quantification of centromeric Haspin-GFP signal intensity, as seen in A, relative to signal intensities of +Haspin-GFP centromeres from three independent experiments (n = 3, 50 centromeres per n) with levels normalized to CENP-A. Error bar represents SD. **, P < 0.01 (Student's t test).

was increased in the pull-down sample compared with Haspin-GFP expressed in XEEs. The molecular weight shift suggests that a posttranslational modified form of Haspin bound onto the SUMOylated CTD. Haspin has been reported to be phosphorylated specifically during mitosis at multiple sites by kinases such as Cdk1 and Plk1 to activate Haspin (Wang et al., 2011; Ghenoiu et al., 2013; Zhou et al., 2014). To determine whether the cell cycle–specific phosphorylation of Haspin contributes to the interaction of Haspin with SUMOylated TOP2A, we performed pull-down assays using either mitotic CSF XEEs or interphase XEEs expressing Haspin-GFP at similar levels, because of difficulty in detecting endogenous Haspin in XEEs and to eliminate the possibility of different Haspin expression levels between mitotic CSF XEEs and interphase XEEs. As a previous study reported (Ghenoiu et al., 2013), exogenous Haspin in mitotic CSF XEEs showed a larger molecular weight than Haspin in interphase XEEs because of mitotic phosphorylation (Fig. 6 A). Haspin-GFP was not detected in the pulled-down fractions from non-SUMOylated TOP2A CTD in CSF or interphase XEEs. However, when CTD-SUMO was used to pull down Haspin, the interphase form of Haspin-GFP was 73% less abundant compared with mitotic CSF Haspin-GFP (Fig. 6 B). This result suggests that, because mitotic Haspin bound much more abundantly to SUMOylated CTD than the interphase form of Haspin, the cell cycle–specific phosphorylation of Haspin can regulate its stable interaction with SUMOylated TOP2A. The initial phosphorylation for Haspin kinase activation is mediated by Cdk1 at threonine 206 in *X. laevis* and threonine 128 in *Homo sapiens* (Ghenoiu et al., 2013; Zhou et al., 2014). T206 acts as a priming site that, when phosphorylated by Cdk1, promotes Plk1 binding for subsequent phosphorylation, which leads to Haspin activation. Because the mitotic phosphorylation of Haspin may play a critical role in its interaction with SUMOylated TOP2A, we examined how a T206A mutation affected Haspin binding to CTD-SUMO (Fig. 6 C). Haspin-GFP WT, T206A, 2-SIM, and a combined T206A/2-SIM mutant were expressed in XEEs separately at similar levels with Haspin-GFP mRNA addition (Fig. 6 D). CTD-SUMO pulled down Haspin 2-SIM at 57% of WT, similar to what was observed in Fig. 2 E, whereas Haspin T206A was pulled down less, at 15% of WT levels (Fig. 6 E). The combined T206A/2-SIM mutant showed slightly lower levels pulled down, at 9% of WT. These results suggest that phosphorylation of T206 greatly contributes to the stable interaction between Haspin and SUMOylated TOP2A, more so than the SIMs, in the in vitro pull-down assays.

Haspin T206 and SIMs regulate its centromeric localization on mitotic chromosomes

Because both T206A and SIM mutations reduced the binding of Haspin to SUMOylated TOP2A CTD, we looked to determine whether these mutations also affected the centromeric localization of Haspin through immunofluorescence using Haspin-GFP WT, T206A, 2-SIM, and T206A/2-SIM expression with the addition of mRNA. To be sure that all four proteins were expressed at similar levels, different mRNA concentrations for

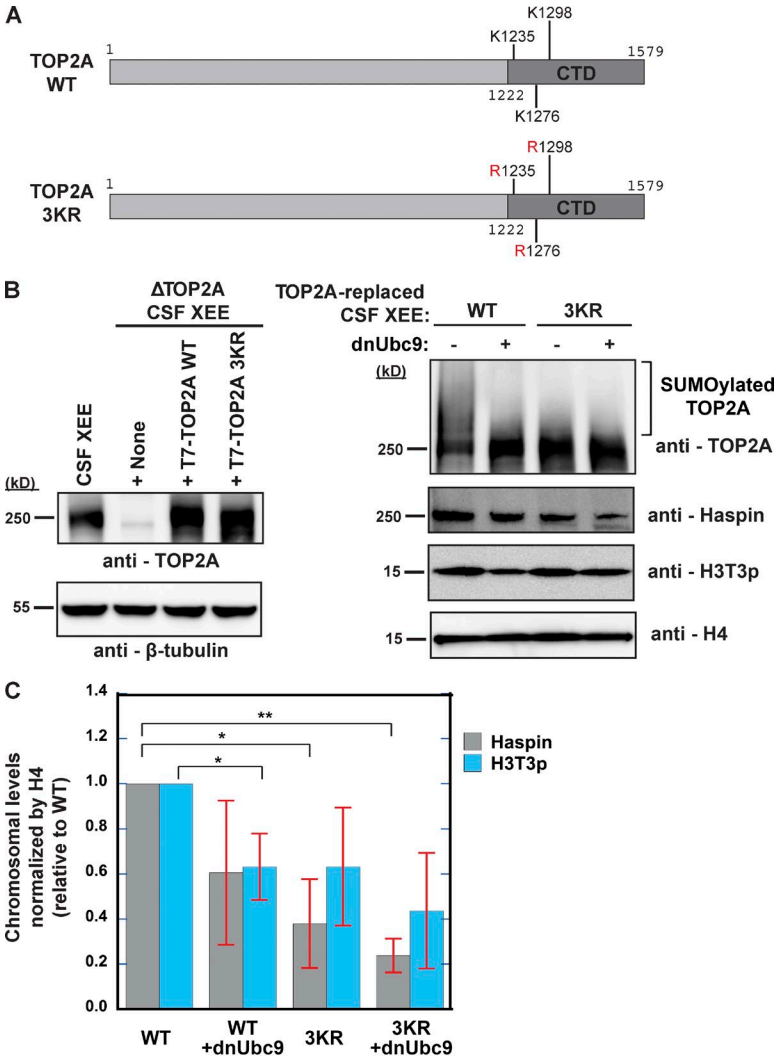

Figure 5. **SUMOylation of TOP2A CTD regulates Haspin binding and H3T3 phosphorylation on mitotic chromosomes.** (A) Schematic representation of the primary structure of *X. laevis* TOP2A. Three lysines indicated in the CTD were mutated to arginine for a TOP2A mutant that could not be SUMOylated in the CTD (3KR). (B) Endogenous TOP2A in CSF XEEs was immunodepleted and replaced with either recombinant full-length T7-TOP2A WT or 3KR (left). β-Tubulin was used as a loading control of TOP2A levels in CSF XEEs. Mitotic chromosomes assembled in TOP2A-replaced CSF XEEs were analyzed by immunoblotting with indicated antibodies (right). Histone H4 was used as a loading control for mitotic chromosomes. (C) Quantification of Haspin and H3T3p levels on the mitotic chromosomes, as seen in B, relative to levels of TOP2A WT chromosomes from three independent experiments (n = 3) with levels normalized to histone H4 levels. Error bar represents SD. *, $P < 0.05$; **, $P < 0.01$ (Student's t test).

each Haspin-GFP form were added into XEEs, and the chromosomes from XEEs with similar expression levels of Haspin-GFP (Fig. 7 A, lanes 2, 5, 8, and 11) were compared. Analysis of the centromeric Haspin-GFP signals showed a clear reduction in the centromeric Haspin localization with the mutant forms. Relative to WT Haspin-GFP levels, Haspin-GFP levels at the centromeres were reduced to 44% in the T206A mutant and 46% in the 2-SIM mutant (Fig. 7 B). Combining the mutations for the T206A/2-SIM mutant reduced the Haspin-GFP signal intensity more at the centromeres, to 23%. This result suggests that T206 phosphorylation and the SIMs contribute to the binding of Haspin to SUMOylated TOP2A CTD through an additive effect.

Altogether, our results suggest that the mitotic chromosomal binding of Haspin at the centromeres can be regulated by its interaction with TOP2A. This interaction occurs at the C-terminal region of TOP2A and is mediated by SUMOylation on TOP2A, Haspin SIMs, and the mitotic phosphorylation on Haspin.

Discussion

Because Aurora B acts as a key mitotic regulator at the centromere during early mitosis, regulation of the recruitment of the CPC is essential for proper mitotic progression. Haspin has been reported to contribute to CPC recruitment (Kelly et al., 2010; Wang et al., 2010). However, the mechanism for the localization of Haspin remained unclear in vertebrates. Our results imply a novel interaction between TOP2A and Haspin for the centromeric Haspin localization that is mediated by two different modifications: (a) the phosphorylation of Haspin required for kinase activation and (b) the SUMOylation of TOP2A C-terminal region (Fig. 8). When both TOP2A and Haspin have been modified, active Haspin is recruited by SUMOylated TOP2A and binds to the vicinity of centromeric histone H3 to phosphorylate H3T3. H3T3p then allows for CPC to localize at the centromeres, whereas Bub1-mediated phosphorylation of H2A T120 also contributes in the recruitment of the CPC via Shugoshin proteins (Kawashima et al., 2010; Yamagishi et al., 2010). However, mutating Haspin T206 is suggested to eliminate both Cdk1- and Plk1-dependent phosphorylation (Ghenoiu et al., 2013). Therefore, it remains unknown whether the phosphorylation of T206 mediated by Cdk1 or the phosphorylation of the sites mediated by Plk1 on Haspin is important for its interaction with TOP2A. It also remains unclear how phosphorylated T206 and potentially other phosphorylated sites on Haspin contribute structurally to the interaction with SUMOylated TOP2A. Without SUMOylation, TOP2A and Haspin do not bind, which suggests that SUMOylation is essential for the two proteins to interact. However, even without the SIM sequences, Haspin can bind to SUMOylated TOP2A, though not

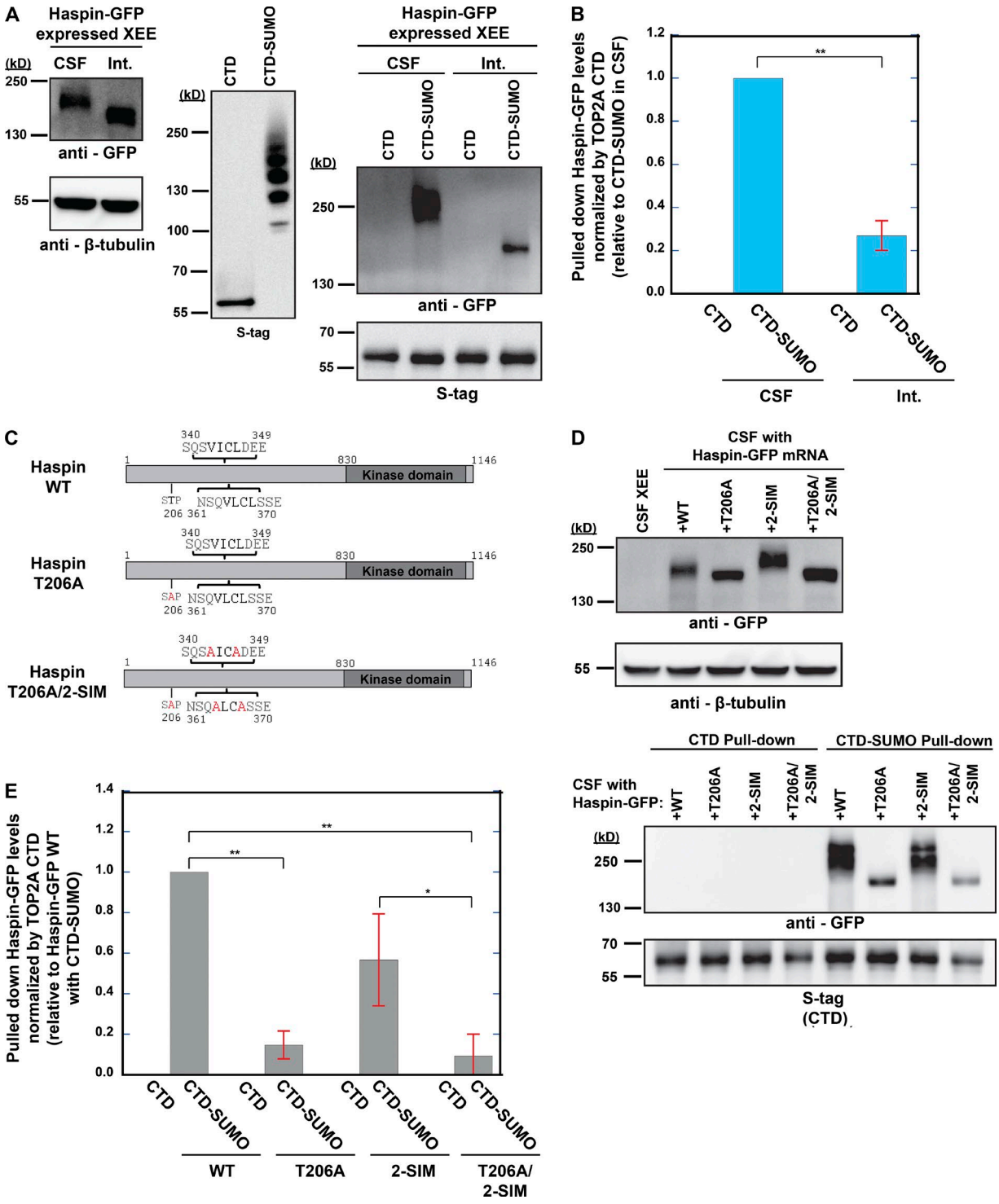

Figure 6. **Cell cycle–dependent Haspin T206 phosphorylation regulates SUMOylated TOP2A CTD–Haspin interaction.** (A) Either CSF XEEs or interphase XEEs (Int.) expressing Haspin-GFP (left) were used in pull-down assays with S-tagged non-SUMOylated (CTD) and SUMOylated CTD (CTD-SUMO) bound to S-agarose beads (middle), and Haspin-GFP binding was analyzed by immunoblotting (right). β-Tubulin was used as a loading control for Haspin-GFP levels in XEEs (loading 0.5% of the volume of XEEs used in each pull-down sample). SENP2-digested S-tagged CTD was used as the loading control for the bait used in the pull-down assay. (B) Quantification of pulled-down Haspin-GFP levels with CTD and CTD-SUMO, as seen in A, relative to levels from the pull-down sample using CSF XEEs with CTD-SUMO from three independent experiments ($n = 3$) with levels normalized to TOP2A CTD levels. Error bar represents SD. **, $P < 0.01$ (Student's *t* test). (C) Schematic representation of *X. laevis* Haspin mutants. Threonine 206 (T206) was mutated to alanine (T206A) to eliminate the mitotic phosphorylation site. T206A/2-SIM indicates the combined T206A and the double SIM mutations. (D) Expressed WT, T206A, 2-SIM, and T206A/2-SIM Haspin-GFP in CSF XEEs (top) were used in pull-down assays with S-tagged CTD and CTD-SUMO bound onto S-agarose beads with Haspin-GFP binding analyzed by immunoblotting (bottom). β-Tubulin was used as a loading control for Haspin-GFP levels in XEEs (loading 0.5% of the volume of XEEs used in each pull-down sample; top). SENP2-digested S-tagged CTD was used as the loading control for the bait used in the pull-down assay (bottom). (E) Quantification of pulled-down Haspin-GFP levels with CTD and CTD-SUMO, as seen in D, relative to Haspin-GFP WT levels of CTD-SUMO from three independent experiments ($n = 3$) with levels normalized to TOP2A CTD levels. Error bar represents SD. *, $P < 0.05$; **, $P < 0.01$ (Student's *t* test).

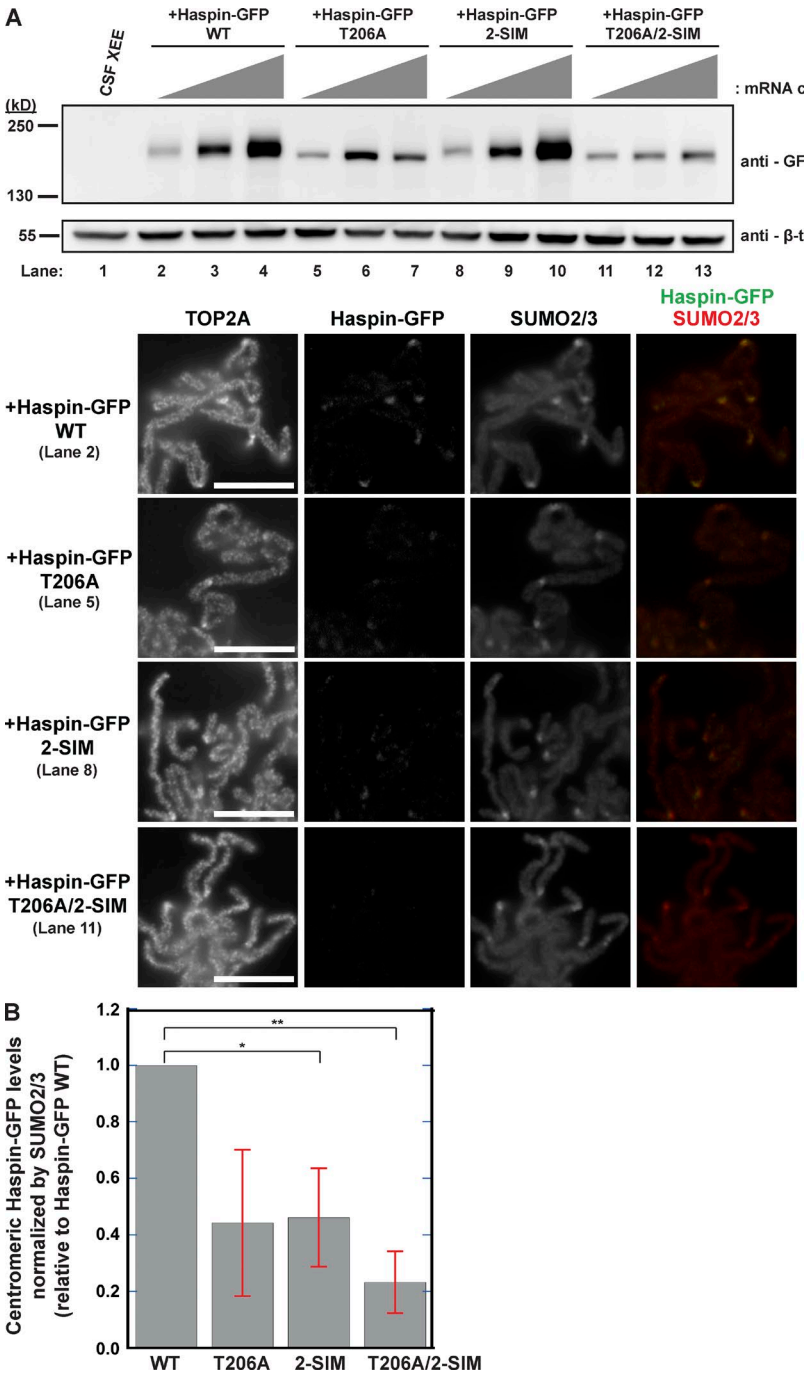

Figure 7. **Haspin SIMs and the phosphorylation of Haspin contribute to its localization at mitotic centromeres.** (A) Mitotic replicated chromosomes prepared from Haspin-GFP–expressing XEEs with different mRNA concentrations of Haspin WT, T206A, 2-SIM, or T206A/2SIM mutant were subjected to immunofluorescence staining. Immunofluorescence staining of chromosomes from XEEs with similar levels of expressed Haspin-GFP is shown and compared (lane 2, WT; lane 5, T206A; lane 8, 2-SIM; and lane 11, T206A/2-SIM). β-Tubulin was used as a loading control for Haspin-GFP levels in CSF XEEs (top). Bars, 10 µm. (B) Chromosomes from XEEs with similar levels of expressed Haspin-GFP were quantified using centromeric Haspin-GFP signal intensity, as seen in A, relative to signal intensities of Haspin-GFP WT from three independent experiments (n = 3, 30 centromeres per n) with levels normalized to SUMO2/3. Error bar represents SD. *, $P < 0.05$; **, $P < 0.01$ (Student's t test).

robustly. This could be because (a) SUMOylation of TOP2A can cause structural change in the CTD, which exposes a surface for phosphorylated Haspin to interact with; (b) phosphorylation of Haspin creates phospho-regulated SIMs (Stehmeier and Muller, 2009) that interact directly with the SUMO protein more tightly; or (c) the phosphorylation-dependent Haspin conformational changes suggested by Ghenoiu et al. (2013) allow it to bind to SUMOylated TOP2A. Future studies involving Haspin phosphorylation site mutants may provide insight on the specific sites that mediate this protein interaction.

Although our results show that the TOP2A CTD SUMOylation can regulate the binding of Haspin on the mitotic chromosomes by using TOP2A 3KR mutant, the addition of dnUbc9 to the XEEs with TOP2A 3KR mutant showed a greater reduction in both Haspin and H3T3p levels on mitotic chromosomes than without the presence of dnUbc9, even though the difference was not statistically significant. This result suggests that although TOP2A SUMOylation can regulate Haspin binding, other SUMOylated proteins on the mitotic chromosomes may function to allow for the binding of Haspin and, thus, also affect H3T3p levels on the chromosomes. It may also be possible that the SUMOylation of TOP2A K660 that we have previously reported contributes to the binding of Haspin on the mitotic chromosomes (Ryu et al., 2010b). Additionally, Haspin binding on the mitotic chromosomes and the centromeric Haspin localization were not completely eliminated when SUMOylation was inhibited or when both T206 and the SIMs were mutated together. This result indicates that there could be other mechanisms

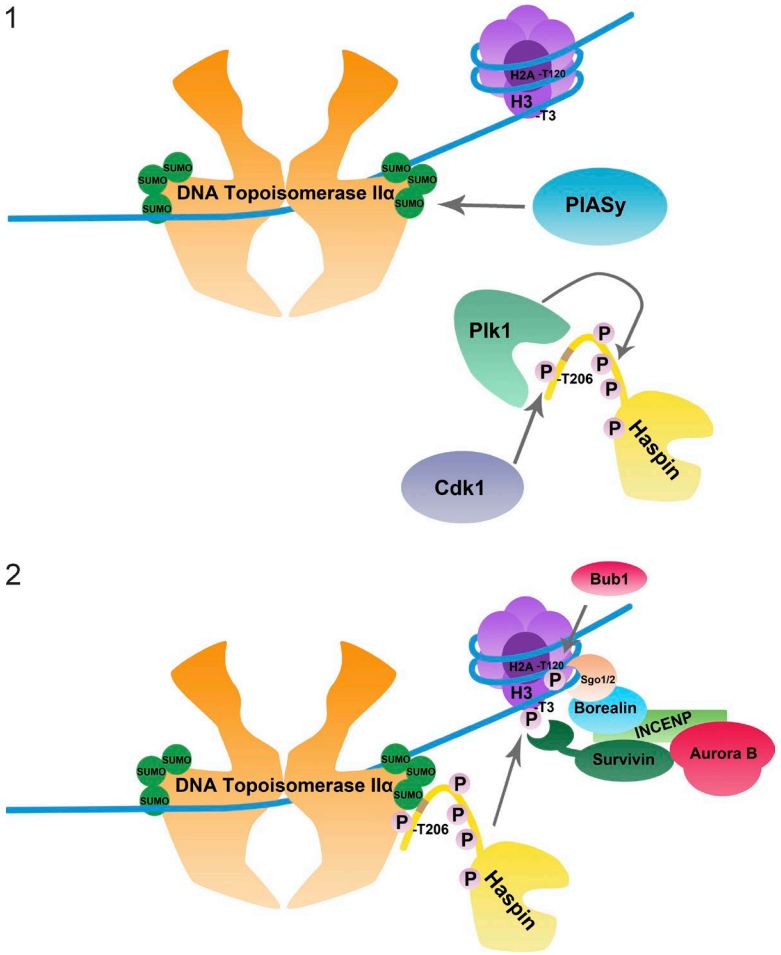

Figure 8. **Model for centromeric Haspin recruitment by DNA topoisomerase IIα.** (1) Centromeric DNA topoisomerase IIα is SUMOylated (S) at the C-terminal domain by SUMO E3 ligase PIASy, whereas Haspin is phosphorylated (P) by Cdk1 at T206 during the onset of mitosis. Plk1 binds to phosphorylated T206 to phosphorylate other sites on Haspin to create active Haspin kinase. (2) SUMOylated topoisomerase IIα recruits active Haspin to the centromere to allow for the phosphorylation of histone H3 (purple) at threonine 3 (T3). Phosphorylated T3 recruits CPC members to the centromere through direct interaction with Survivin. H2A (dark purple) T120 phosphorylation mediated by Bub1 additionally contributes to the recruitment of CPC members to the centromere through the binding of Shugoshin 1/2 (Sgo1/2) that interacts with Borealin.

for Haspin binding on the mitotic chromosomes that are independent of SUMOylation, such as through the interaction with the cohesin cofactor Pds5 (Yamagishi et al., 2010).

An analysis in budding yeast, concurrently reported with this study, shows that H3T3p-mediated Aurora B (Ipl1 in budding yeast) localization at the mitotic centromeres is conserved, and mislocalization of Aurora B is observed in yeast with a truncated form of TOP2 lacking the CTD (unpublished data). Rescue of the H3T3p-dependent Aurora B localization in the truncated TOP2 mutant yeast by H3T3E substitution supports the conserved role of the CTD in the regulation of Aurora B localization in eukaryotes. Previous study has shown that TOP2A contributes in the regulation of Aurora B activity at the centromeres in somatic cells with TOP2 inhibitor treatment (Coelho et al., 2008). TOP2 inhibitors have also been known to increase the SUMOylation of TOP2A in mitotic HeLa cells (Agostinho et al., 2008). Our results suggest that the SUMOylation-dependent regulation of Haspin may explain the molecular mechanism of the TOP2 inhibitor–dependent regulation of Aurora B. In addition, a recent study indicated that specific mutations of TOP2 in budding yeast that obstruct the strand-passaging enzymatic reaction of TOP2 at different enzymatic steps can induce mitotic checkpoint activation (Furniss et al., 2013). This mitotic checkpoint activation required the C-terminal region of TOP2, suggesting that TOP2 CTD can provide a signal to the mitotic checkpoint machinery. An intriguing question for the future is whether the SUMOylated TOP2A CTD and Haspin interaction is involved in the checkpoint activation caused by the strand-passaging reaction mutant TOP2.

Materials and methods

DNA constructs, site-directed mutagenesis, recombinant protein expression, and antibodies

For recombinant full-length *X. laevis* TOP2A proteins, cDNAs were subcloned into a pPIC3.5 vector (Thermo Fisher Scientific) that had a calmodulin-binding protein (CBP)–T7 tag sequence and were expressed in the GS115 strain of *Pichia pastoris* yeast. CBP-T7 tagged TOP2A proteins were extracted by grinding frozen yeast cells with dry ice, followed by the addition of lysis buffer (150 mM NaCl, 2 mM $CaCl_2$, 1 mM $MgCl_2$, and 30 mM Hepes, pH 7.8), and purified by calmodulin-agarose (GE Healthcare) affinity chromatography and by anion exchange column (GE Healthcare) as previously described (Ryu et al., 2010a,b). TOP2A CTD (aa 1,222–1,579) was subcloned into pET30a (EMD Millipore) and SENP2 catalytic domain (CD; aa 363–589), and PIASy cDNAs were subcloned into pET28a vectors (EMD Millipore) with an N-terminal His tag. For E1 complex (Aos1/Uba2 heterodimer), Uba2 and Aos1 cDNAs were subcloned into pRSF Duet vector (EMD Millipore) and expressed together in *Escherichia coli*. Both WT and dominant-negative forms of Ubc9 (dnUbc9-C93S/L97S) were subcloned into pT7-7 vectors (from M. Dasso, National Institutes of Health, Bethesda, MD; Tabor and Richardson, 1985), and SUMO2-GG was subcloned into pGEX4T-1 (GE Healthcare) with an N-terminal GST tag. All proteins were expressed in BL21 (DE3) or Rosetta 2 (DE3) bacteria at either 15°C in 2× YT medium containing 5% glycerol and 2.5% ethanol (for TOP2A CTD, SENP2 catalytic domain, PIASy, and E1 complex) or 30°C in 2× YT medium (for Ubc9 and SUMO2-GG). Proteins with His-6 tag (TOP2A CTD, PIASy, and

SENP2 CD) were extracted by lysing cells in buffer (500 mM NaCl, 1 mM $MgCl_2$, 25 mM Hepes, pH 7.8, 5% glycerol, 1 mM PMSF, and 0.5% Triton X-100) with 0.1 mg/ml lysozyme (Sigma-Aldrich). His-6–tagged proteins were purified using Cobalt affinity beads (Talon Beads; Takara Bio Inc.) from soluble fractions after centrifugation at 25,000 *g* for 40 min. Proteins were eluted with imidazole, and imidazole-eluted fractions were further separated by ion-exchange columns. For E1 complex purification, cells were lysed as noted earlier except with 150 mM NaCl concentration. The E1 complex–containing imidazole elutions were loaded onto a SUMO1 affinity column (GST-SUMO1-GG conjugated to NHS-Sepharose; GE Healthcare) in the presence of ATP, and bound E1 complex was eluted by DTT elution buffer (100 mM NaCl, 1 mM $MgCl_2$, 30 mM Tris, pH 8.8, 5% glycerol, and 10 mM DTT). E1 complex–containing DTT-eluted fractions were further purified by anion exchange column. GST-SUMO2-GG was extracted from *E. coli* cells by the lysis method mentioned earlier and captured on glutathione-Sepharose beads (GE Healthcare). Bound beads were incubated with thrombin to cleave the GST tag to elute untagged SUMO2-GG. Eluted SUMO2-GG was further purified by anion exchange column followed by Sephacryl S-100 gel filtration (GE Healthcare). Ubc9 proteins were extracted by sonication in 50 mM NaCl lysis buffer. The soluble fraction after centrifugation was loaded onto the anion exchange column. Collected Ubc9 proteins were separated by cation exchange column followed by Sephacryl S-100 gel filtration. All proteins were concentrated with buffer exchanged to 100 mM NaCl, 1 mM $MgCl_2$, 20 mM Hepes, pH 7.8, 5% glycerol, and 0.5 mM tris(2-carboxyethyl)phosphine with a centrifugal concentrator (Amicon Ultra; Thermo Fisher Scientific). The protein concentrations were measured using the Bradford method (Bio-Rad Laboratories), with BSA as the standard. Purified proteins were snap-frozen with liquid nitrogen and stored at −80°C.

X. laevis Haspin cloned into a pTGFC70 plasmid with a C-terminal GFP tag and a 3′-UTR sequence of xKid was a gift from H. Funabiki (Rockefeller University, New York, NY). SIMs were predicted using the GPS-SUMO prediction program (Xue et al., 2006). Mutations in the SIMs at aa 343–346 (VICL to AICA) and aa 364–367 (VLCL to ALCA) and the T206A (threonine to alanine) mutation were generated by site-directed mutagenesis using a QuikChange II XL kit (Agilent Technologies) according to the manufacturer's protocol and verified by DNA sequencing. WT and mutant Haspin mRNA were obtained by in vitro transcription reaction with mMESSAGE mMACHINE SP6 kit (Thermo Fisher Scientific) from pTGFC70 plasmid as previously described (Kelly et al., 2010; Ghenoiu et al., 2013). The pTGFC70 plasmids of WT and mutant Haspin-GFP were first linearized with NotI restriction enzyme digestion. Linearized pTGFC70 plasmids were incubated with the mMESSAGE mMACHINE SP6 kit transcription mixture for 3 h at 37°C to synthesize mRNA. The transcribed mRNAs were precipitated in LiCl for recovery and dissolved in nuclease-free H_2O.

Antibodies used for the study are as follows. For immunoblotting, rabbit anti-SUMO2/3 polyclonal antibody (1:1,000) and rabbit polyclonal antibody against the TOP2A C-terminus region (aa 1,358–1,579; 1:1,000) were prepared as previously described (Azuma et al., 2003; Ryu and Azuma, 2010; Ryu et al., 2010b). Anti–Aurora B kinase rabbit polyclonal antibody (1:1,000) was prepared with full-length *X. laevis* Aurora B as the antigen. Rabbit anti-Haspin polyclonal antibody for *X. laevis* was a gift of H. Funabiki (Kelly et al., 2010). Rabbit polyclonal antibodies of anti-Pds5a and anti-Pds5b for *X. laevis* were a gift of T. Hirano (Institute of Physical and Chemical Research, Saitama, Japan; Losada et al., 2005). Commercial antibodies used for immunoblotting analysis were mouse monoclonal anti-GFP (JL-8, 1:1,000; Takara Bio Inc.), rabbit monoclonal anti–Aurora B kinase T232 phosphorylation (T248 in *X. laevis*, 1:1,000; Cell Signaling Technology), rabbit polyclonal anti–histone H3 (1:1,000; Cell Signaling Technology), rabbit polyclonal anti–histone H4 (1:1,000; Abcam), rabbit polyclonal anti-H3T3p (1:1,000; Abcam), S-protein-HRP (1:2,000; EMD Millipore), and mouse monoclonal anti–β-tubulin (1:1,000; Sigma-Aldrich). For immunofluorescence staining, anti-SUMO2/3 guinea pig polyclonal antibody (1:500) and chicken polyclonal anti–*X. laevis* CENP-A (1:500) were prepared as previously described (Azuma et al., 2003; Ryu et al., 2010a,b; Ryu and Azuma, 2010), and anti–Aurora B rabbit polyclonal antibody (1:500) was used. Commercial antibodies used for immunofluorescence analysis were mouse anti–topoisomerase II monoclonal antibody (1:1,000; MBL International) and rabbit polyclonal anti–histone H3T3p (1:25,000; Abcam). Primary antibodies were visualized by fluorescence-labeled secondary antibodies (Thermo Fisher Scientific): goat anti–mouse IgG Alexa Fluor 488 (1:500), goat anti–rabbit IgG Alexa Fluor 568 (1:500), goat anti–guinea pig IgG Alexa Fluor 678 (1:500), and goat anti–chicken IgG Alexa Fluor 488 (1:500).

XEEs, immunodepletion/add-back assay, and pull-down assays

Low-speed extracts of *X. laevis* eggs arrested in metaphase with cytostatic factor (CSF XEEs) and demembraned sperm nuclei were prepared according to standard protocols (Murray, 1991; Kornbluth and Evans, 2001). Immunodepletions of endogenous TOP2A were performed with protein A–conjugated magnetic beads (Thermo Fisher Scientific; Arnaoutov and Dasso, 2003). Equal volumes of rabbit anti-TOP2A antibody (1 mg/ml) and protein A Dynabeads suspension were incubated to capture the antibodies on Dynabeads. Anti-TOP2A–captured beads were blocked with 5% BSA containing CSF-XB (100 mM KCl, 0.1 mM $CaCl_2$, 2 mM $MgCl_2$, 5 mM EGTA, 50 mM sucrose, and 10 mM Hepes, pH 7.8). To reach greater than 99% depletion of TOP2A from XEEs, we used anti-TOP2A–captured Dynabeads from initial Dynabead suspension at a ratio of 1.1 µl suspension to 1 µl XEEs (i.e., 440 µl suspension of anti-TOP2A Dynabeads were used for immunodepletion in 400 µl XEEs in Fig. 5). The XEE/Dynabeads mixture was incubated for 15 min at RT followed by 15-min incubation on ice. For add-back experiments, purified recombinant T7-TOP2A proteins were added to immunodepleted extracts at levels similar to the endogenous TOP2A, which was confirmed by immunoblotting. Chromosome isolations were performed as previously reported (Azuma, 2009). For chromosome isolation, interphase extract was first obtained by releasing metaphase-arrested XEEs with 0.6 mM $CaCl_2$. Demembranated sperm nuclei were incubated in interphase XEEs at 6,000 sperm nuclei/µl, and an equal volume of CSF XEEs was added to induce the onset of mitosis. Mitotic SUMOylation was inhibited by the addition of 150 ng/µl dnUbc9 to the interphase XEEs as well as the CSF XEEs right before the two XEEs were combined for the induction of mitosis from interphase. After incubation, XEEs were diluted by three times their volume with 0.5× CSF-XB supplemented with 18 mM β-glycerophosphate, 0.25% Triton X-100, 10 mg/ml protease inhibitors (leupeptin, pepstatin, and chymostatin; EMD Millipore), and 0.2 µM okadaic acid (EMD Millipore). Diluted XEEs were layered onto dilution buffer containing 35% glycerol and centrifuged at 10,000 *g* for 5 min at 4°C. Precipitated chromosomes were boiled in SDS-PAGE sample buffer, and the extracted proteins were subjected to immunoblotting with antibodies. Immunoblotting signals were acquired with Image Station 4000R (Carestream Health), and the signal levels were quantified by ImageJ software. Relative levels were calculated by measuring the signal levels of each protein band, normalizing values to the loading controls indicated in each figure, and taking the mean and SD of three independent experiments for each assay. Statistical significance of the difference was calculated by *t* test of the means.

The XEE pull-down assays were performed as described previously with 10 mM iodoacetamide addition in buffers to prevent

deSUMOylation activity in the XEEs (Ryu and Azuma, 2010). XEEs were diluted by two times their volume with PD buffer (20 mM sodium phosphate, pH 7.8, 18 mM β-glycerol phosphate, pH 7.5, 5 mM $MgCl_2$, 50 mM NaCl, 5% glycerol, 1 mM DTT, and 10 mM iodoacetamide), and diluted XEEs were centrifuged at 25,000 *g* for 45 min at 4°C. An equal volume of the PD buffer supplemented with 0.2% Tween 20 and 0.2% Triton X-100 was added to the supernatants and incubated with S-tagged TOP2A CTD-bound or SUMOylated TOP2A CTD-bound S-agarose beads for 1 h at RT. After washing with PD buffer, the beads were incubated in the dilution buffer (20 mM sodium phosphate, pH 7.8, 18 mM β-glycerol phosphate, pH 7.5, 5 mM $MgCl_2$, 50 mM NaCl, and 5% glycerol) containing 35 µg/ml SENP2-CD for 45 min at RT to cleave conjugated SUMO2 from TOP2A CTD and dissociate pulled-down proteins from the beads. SDS-PAGE samples were prepared by adding a half volume of 3× SDS-PAGE sample buffer to the bead suspension. All samples were separated on 8–16% Tris-glycine gels (Thermo Fisher Scientific) by SDS-PAGE and analyzed with silver staining or immunoblotting. For the preparation of samples for LC/MS-MS analysis, pull-down samples and the soluble fractions were isolated using spin columns, washed with urea, and precipitated with trichloroacetic acid. Samples were subjected to LC/MS-MS analysis for protein identification (performed by S.P. Gygi, Harvard Medical School, Boston, MA). In the case of pull-down assays with Haspin-GFP–expressing XEEs, interphase XEEs with 10 ng/µl Haspin-GFP mRNA were incubated for 150 min at RT and then returned to mitotic phase by adding an equal volume of CSF XEEs or kept in interphase XEEs for the pull-down experiment in Fig. 6 A. Protein expression levels in XEEs after incubation with mRNA were checked through immunoblotting and adjusted accordingly with additional volumes of the original CSF XEEs or interphase XEEs to achieve similar protein expression concentrations before being used for pull-down assays. Immunoblotting signals were acquired by Image Station 4000R (Carestream Health), and signal levels were quantified by ImageJ software. Relative levels were calculated by measuring the signal levels of each protein band, normalizing the values to the recombinant TOP2A CTD levels, and taking the mean and SD of three independent experiments for each assay. Statistical significance of the difference was calculated by *t* test of the means.

Immunofluorescence analysis of chromosomes

The mitotic chromosomes used for the immunofluorescence analysis were prepared as previously described (Azuma et al., 2005). Replicated mitotic chromosomes were prepared by incubating demembranated sperm chromatin at 1,000 sperm nuclei/µl in interphase XEEs by adding 0.6 mM $CaCl_2$, followed by the induction of mitosis with the addition of an equal volume of CSF XEEs. To inhibit SUMOylation, 150 ng/µl dnUbc9 was added to both the interphase XEEs and CSF XEEs before they were combined to induce the onset of mitosis. XEE-containing mitotic chromosomes were diluted by three times their volume with IF-dilution buffer (0.5× CSF-XB containing 18 mM β-glycerophosphate and 250 mM sucrose) and an equal volume of fixation buffer (IF-dilution buffer with 4% *p*-formaldehyde) followed by incubation for 10 min at RT. Fixed samples were layered on top of 8 ml of 40% glycerol cushion in glass tubes with coverslips. The chromosomes were spun down onto the coverslips by centrifuging at 6,000 *g* for 20 min at RT. Chromosomes on the coverslips were postfixed with 1.6% *p*-formaldehyde in PBS for 5 min at RT. The specimens were blocked with PBS containing 5% BSA and 2.5% cold-fish gelatin and subjected to immunostaining with the antibodies. The localization of Haspin on mitotic chromosomes was observed by GFP signals from exogenously expressed Haspin-GFP prepared from mRNA addition to XEEs (Ghenoiu et al., 2013). For Haspin-GFP expression from mRNA, Haspin-GFP mRNA was incubated in interphase XEEs at RT for 60 min at a concentration of 20 ng/µl (Fig. 3 A) or at multiple concentrations of 20, 40, and 60 ng/µl (Fig. 7 A). Afterward, demembraned sperm nuclei were added to allow for DNA replication. After the completion of DNA replication, an equal volume of CSF XEEs was added and incubated for 45 min for mitotic CSF XEEs with Haspin-GFP. DNA was stained with Hoechst 33342 dye (EMD Millipore), and the samples were mounted using Vectashield H-1000 medium (Vector Laboratories). All images were acquired using the Nikon Plan Apo 100×/1.4 oil objective lens on a TE2000-U microscope (Nikon) with a Retiga SRV CCD camera (QImaging) operated by Volocity imaging software (PerkinElmer) at RT. Photoshop CS6 (Adobe) was used to process the obtained images from Volocity to show the signal intensities by adjusting overall intensity range levels equally within independent experiments without any gamma adjustments. Images were cropped and the resolution was adjusted to fit journal policy. Quantification of fluorescent signals was through ImageJ and Photoshop CS6 by measuring the signal intensity around CENP-A or SUMO2/3. Relative intensities of signals from indicated antibodies or GFP were normalized to CENP-A or SUMO2/3 signals. The means of the signal intensities from multiple centromeres were calculated for each independent experiment, and the mean and SD of three independent experiments were determined for each assay. Statistical significance of the difference was calculated by *t* test of the means.

In vitro SUMOylation reaction

In vitro SUMOylation reaction was done by incubating 40 nM Aos1/Uba2, 80 nM Ubc9, 40 nM PIASy, 24 µM SUMO2-GG, 4 µM S-tagged TOP2A CTD, and 2.5 mM ATP for 2 h at 25°C before binding onto S-agarose beads (EMD Millipore) overnight in 4°C for use in pull-down assays. Non-SUMOylated CTD was prepared by incubating with the aforementioned mixture but without ATP.

Online supplemental material

Table S1 shows the summarized list of proteins that were pulled down specifically with SUMOylated TOP2A CTD and identified through LC-MS/MS analysis. Fig. S1 is the pull-down assay using recombinant S-tagged TOP2A CTD and CTD-SUMO through in vitro SUMOylation assay with SUMO2, which were bound to S-agarose beads and incubated in CSF XEEs. CTD-bound and CTD-SUMO-bound agarose beads were isolated, digested by SENP2 CD, and analyzed by immunoblotting for Pds5a and Pds5b. Neither Pds5a nor Pds5b were pulled down with either TOP2A CTD or SUMOylated TOP2A CTD. Fig. S2 shows the mitotic replicated centromeres cropped from Fig. 3 C to focus on a single pair of centromeres and signals of CENP-A, SUMO2/3, and H3T3p. A reduction in H3T3p signal intensity at the centromere is seen when dnUbc9 is added to inhibit SUMOylation. Online supplemental material is available at http://www.jcb.org/cgi/content/full/jcb.201511079/DC1.

Acknowledgments

We thank D. Clarke of University of Minnesota, M. Dasso of National Institutes of Health, and H. Funabiki of Rockefeller University for their critical discussion of this project and H. Funabiki for the pTGFC70 plasmid and rabbit polyclonal anti-Haspin antibody. We also thank T. Hirano of Institute of Physical and Chemical Research (RIKEN) for the rabbit polyclonal anti-Pds5a and anti-Pds5b antibodies.

This project was supported (Y. Azuma and M.M. Yoshida) by National Institutes of Health/National Institute of General Medical Sciences grant GM80278 and bridge funding from the University of Kansas. It

is supported in part by a general research fund from the University of Kansas (#2301743), and is currently supported by National Institutes of Health/National Institute of General Medical Sciences grant GM112793.

The authors declare no competing financial interests.

Submitted: 23 November 2015
Accepted: 6 April 2016

References

Adams, R.R., S.P. Wheatley, A.M. Gouldsworthy, S.E. Kandels-Lewis, M. Carmena, C. Smythe, D.L. Gerloff, and W.C. Earnshaw. 2000. INC ENP binds the Aurora-related kinase AIRK2 and is required to target it to chromosomes, the central spindle and cleavage furrow. *Curr. Biol.* 10:1075–1078. http://dx.doi.org/10.1016/S0960-9822(00)00673-4

Agostinho, M., V. Santos, F. Ferreira, R. Costa, J. Cardoso, I. Pinheiro, J. Rino, E. Jaffray, R.T. Hay, and J. Ferreira. 2008. Conjugation of human topoisomerase 2 alpha with small ubiquitin-like modifiers 2/3 in response to topoisomerase inhibitors: cell cycle stage and chromosome domain specificity. *Cancer Res.* 68:2409–2418. http://dx.doi.org/10.1158/0008-5472.CAN-07-2092

Arnaoutov, A., and M. Dasso. 2003. The Ran GTPase regulates kinetochore function. *Dev. Cell.* 5:99–111. http://dx.doi.org/10.1016/S1534-5807(03)00194-1

Azuma, Y. 2009. Analysis of SUMOylation of topoisomerase IIalpha with *Xenopus* egg extracts. *Methods Mol. Biol.* 582:221–231. http://dx.doi.org/10.1007/978-1-60761-340-4_17

Azuma, Y., A. Arnaoutov, and M. Dasso. 2003. SUMO-2/3 regulates topoisomerase II in mitosis. *J. Cell Biol.* 163:477–487. http://dx.doi.org/10.1083/jcb.200304088

Azuma, Y., A. Arnaoutov, T. Anan, and M. Dasso. 2005. PIASy mediates SUMO-2 conjugation of topoisomerase-II on mitotic chromosomes. *EMBO J.* 24:2172–2182. http://dx.doi.org/10.1038/sj.emboj.7600700

Bachant, J., A. Alcasabas, Y. Blat, N. Kleckner, and S.J. Elledge. 2002. The SUMO-1 isopeptidase Smt4 is linked to centromeric cohesion through SUMO-1 modification of DNA topoisomerase II. *Mol. Cell.* 9:1169–1182. http://dx.doi.org/10.1016/S1097-2765(02)00543-9

Biggins, S., N. Bhalla, A. Chang, D.L. Smith, and A.W. Murray. 2001. Genes involved in sister chromatid separation and segregation in the budding yeast *Saccharomyces cerevisiae*. *Genetics.* 159:453–470.

Carmena, M., M. Wheelock, H. Funabiki, and W.C. Earnshaw. 2012. The chromosomal passenger complex (CPC): From easy rider to the godfather of mitosis. *Nat. Rev. Mol. Cell Biol.* 13:789–803. http://dx.doi.org/10.1038/nrm3474

Carretero, M., M. Ruiz-Torres, M. Rodríguez-Corsino, I. Barthelemy, and A. Losada. 2013. Pds5B is required for cohesion establishment and Aurora B accumulation at centromeres. *EMBO J.* 32:2938–2949. http://dx.doi.org/10.1038/emboj.2013.230

Cheeseman, I.M., J.S. Chappie, E.M. Wilson-Kubalek, and A. Desai. 2006. The conserved KMN network constitutes the core microtubule-binding site of the kinetochore. *Cell.* 127:983–997. http://dx.doi.org/10.1016/j.cell.2006.09.039

Cimini, D., X. Wan, C.B. Hirel, and E.D. Salmon. 2006. Aurora kinase promotes turnover of kinetochore microtubules to reduce chromosome segregation errors. *Curr. Biol.* 16:1711–1718. http://dx.doi.org/10.1016/j.cub.2006.07.022

Coelho, P.A., J. Queiroz-Machado, A.M. Carmo, S. Moutinho-Pereira, H. Maiato, and C.E. Sunkel. 2008. Dual role of topoisomerase II in centromere resolution and aurora B activity. *PLoS Biol.* 6:e207. http://dx.doi.org/10.1371/journal.pbio.0060207

Dai, J., S. Sultan, S.S. Taylor, and J.M. Higgins. 2005. The kinase Haspin is required for mitotic histone H3 Thr 3 phosphorylation and normal metaphase chromosome alignment. *Genes Dev.* 19:472–488. http://dx.doi.org/10.1101/gad.1267105

DeLuca, J.G., W.E. Gall, C. Ciferri, D. Cimini, A. Musacchio, and E.D. Salmon. 2006. Kinetochore microtubule dynamics and attachment stability are regulated by Hec1. *Cell.* 127:969–982. http://dx.doi.org/10.1016/j.cell.2006.09.047

Furniss, K.L., H.J. Tsai, J.A. Byl, A.B. Lane, A.C. Vas, W.S. Hsu, N. Osheroff, and D.J. Clarke. 2013. Direct monitoring of the strand passage reaction of DNA topoisomerase II triggers checkpoint activation. *PLoS Genet.* 9:e1003832. http://dx.doi.org/10.1371/journal.pgen.1003832

Gassmann, R., A. Carvalho, A.J. Henzing, S. Ruchaud, D.F. Hudson, R. Honda, E.A. Nigg, D.L. Gerloff, and W.C. Earnshaw. 2004. Borealin: A novel chromosomal passenger required for stability of the bipolar mitotic spindle. *J. Cell Biol.* 166:179–191. http://dx.doi.org/10.1083/jcb.200404001

Ghenoiu, C., M.S. Wheelock, and H. Funabiki. 2013. Autoinhibition and Polo-dependent multisite phosphorylation restrict activity of the histone H3 kinase haspin to mitosis. *Mol. Cell.* 52:734–745. http://dx.doi.org/10.1016/j.molcel.2013.10.002

Häkli, M., U. Karvonen, O.A. Jänne, and J.J. Palvimo. 2005. SUMO-1 promotes association of SNURF (RNF4) with PML nuclear bodies. *Exp. Cell Res.* 304:224–233. http://dx.doi.org/10.1016/j.yexcr.2004.10.029

Hecker, C.M., M. Rabiller, K. Haglund, P. Bayer, and I. Dikic. 2006. Specification of SUMO1- and SUMO2-interacting motifs. *J. Biol. Chem.* 281:16117–16127. http://dx.doi.org/10.1074/jbc.M512757200

Holm, C., T. Goto, J.C. Wang, and D. Botstein. 1985. DNA topoisomerase II is required at the time of mitosis in yeast. *Cell.* 41:553–563. http://dx.doi.org/10.1016/S0092-8674(85)80028-3

Jeyaprakash, A.A., C. Basquin, U. Jayachandran, and E. Conti. 2011. Structural basis for the recognition of phosphorylated histone h3 by the survivin subunit of the chromosomal passenger complex. *Structure.* 19:1625–1634. http://dx.doi.org/10.1016/j.str.2011.09.002

Kaitna, S., M. Mendoza, V. Jantsch-Plunger, and M. Glotzer. 2000. Incenp and an aurora-like kinase form a complex essential for chromosome segregation and efficient completion of cytokinesis. *Curr. Biol.* 10:1172–1181. http://dx.doi.org/10.1016/S0960-9822(00)00721-1

Kawashima, S.A., Y. Yamagishi, T. Honda, K. Ishiguro, and Y. Watanabe. 2010. Phosphorylation of H2A by Bub1 prevents chromosomal instability through localizing shugoshin. *Science.* 327:172–177. http://dx.doi.org/10.1126/science.1180189

Kelly, A.E., C. Ghenoiu, J.Z. Xue, C. Zierhut, H. Kimura, and H. Funabiki. 2010. Survivin reads phosphorylated histone H3 threonine 3 to activate the mitotic kinase Aurora B. *Science.* 330:235–239. http://dx.doi.org/10.1126/science.1189505

Kornbluth, S., and E.K. Evans. 2001. Analysis of apoptosis using *Xenopus* egg extracts. Curr Protoc Cell Biol. Chapter 11:Unit 11.12. http://dx.doi.org/10.1002/0471143030.cb1112s09

Kumagai, A., and W.G. Dunphy. 2000. Claspin, a novel protein required for the activation of Chk1 during a DNA replication checkpoint response in *Xenopus* egg extracts. *Mol. Cell.* 6:839–849. http://dx.doi.org/10.1016/S1097-2765(05)00092-4

Lan, W., X. Zhang, S.L. Kline-Smith, S.E. Rosasco, G.A. Barrett-Wilt, J. Shabanowitz, D.F. Hunt, C.E. Walczak, and P.T. Stukenberg. 2004. Aurora B phosphorylates centromeric MCAK and regulates its localization and microtubule depolymerization activity. *Curr. Biol.* 14:273–286. http://dx.doi.org/10.1016/j.cub.2004.01.055

Losada, A., T. Yokochi, and T. Hirano. 2005. Functional contribution of Pds5 to cohesin-mediated cohesion in human cells and *Xenopus* egg extracts. *J. Cell Sci.* 118:2133–2141. http://dx.doi.org/10.1242/jcs.02355

Luo, K., J. Yuan, J. Chen, and Z. Lou. 2009. Topoisomerase IIalpha controls the decatenation checkpoint. *Nat. Cell Biol.* 11:204–210. http://dx.doi.org/10.1038/ncb1828

Mao, Y., S.D. Desai, and L.F. Liu. 2000. SUMO-1 conjugation to human DNA topoisomerase II isozymes. *J. Biol. Chem.* 275:26066–26073. http://dx.doi.org/10.1074/jbc.M001831200

Murray, A.W. 1991. Cell cycle extracts. *Methods Cell Biol.* 36:581–605. http://dx.doi.org/10.1016/S0091-679X(08)60298-8

Nitiss, J.L. 2009. DNA topoisomerase II and its growing repertoire of biological functions. *Nat. Rev. Cancer.* 9:327–337. http://dx.doi.org/10.1038/nrc2608

Petsalaki, E., T. Akoumianaki, E.J. Black, D.A. Gillespie, and G. Zachos. 2011. Phosphorylation at serine 331 is required for Aurora B activation. *J. Cell Biol.* 195:449–466. http://dx.doi.org/10.1083/jcb.201104023

Pinsky, B.A., C. Kung, K.M. Shokat, and S. Biggins. 2006. The Ipl1-Aurora protein kinase activates the spindle checkpoint by creating unattached kinetochores. *Nat. Cell Biol.* 8:78–83. http://dx.doi.org/10.1038/ncb1341

Rosendorff, A., S. Sakakibara, S. Lu, E. Kieff, Y. Xuan, A. DiBacco, Y. Shi, Y. Shi, and G. Gill. 2006. NXP-2 association with SUMO-2 depends on lysines required for transcriptional repression. *Proc. Natl. Acad. Sci. USA.* 103:5308–5313. http://dx.doi.org/10.1073/pnas.0601066103

Ryu, H., and Y. Azuma. 2010. Rod/Zw10 complex is required for PIASy-dependent centromeric SUMOylation. *J. Biol. Chem.* 285:32576–32585. http://dx.doi.org/10.1074/jbc.M110.153817

Ryu, H., G. Al-Ani, K. Deckert, D. Kirkpatrick, S.P. Gygi, M. Dasso, and Y. Azuma. 2010a. PIASy mediates SUMO-2/3 conjugation of poly(ADP-ribose) polymerase 1 (PARP1) on mitotic chromosomes. *J. Biol. Chem.* 285:14415–14423. http://dx.doi.org/10.1074/jbc.M109.074583

Ryu, H., M. Furuta, D. Kirkpatrick, S.P. Gygi, and Y. Azuma. 2010b. PIASy-dependent SUMOylation regulates DNA topoisomerase IIalpha activity. *J. Cell Biol.* 191:783–794. http://dx.doi.org/10.1083/jcb.201004033

Ryu, H., M.M. Yoshida, V. Sridharan, A. Kumagai, W.G. Dunphy, M. Dasso, and Y. Azuma. 2015. SUMOylation of the C-terminal domain of DNA topoisomerase IIα regulates the centromeric localization of Claspin. *Cell Cycle.* 14:2777–2784. http://dx.doi.org/10.1080/15384101.2015.1066537

Song, J., L.K. Durrin, T.A. Wilkinson, T.G. Krontiris, and Y. Chen. 2004. Identification of a SUMO-binding motif that recognizes SUMO-modified proteins. *Proc. Natl. Acad. Sci. USA.* 101:14373–14378. http://dx.doi.org/10.1073/pnas.0403498101

Song, J., Z. Zhang, W. Hu, and Y. Chen. 2005. Small ubiquitin-like modifier (SUMO) recognition of a SUMO binding motif: A reversal of the bound orientation. *J. Biol. Chem.* 280:40122–40129. http://dx.doi.org/10.1074/jbc.M507059200

Sridharan, V., H. Park, H. Ryu, and Y. Azuma. 2015. SUMOylation regulates polo-like kinase 1-interacting checkpoint helicase (PICH) during mitosis. *J. Biol. Chem.* 290:3269–3276. http://dx.doi.org/10.1074/jbc.C114.601906

Stehmeier, P., and S. Muller. 2009. Phospho-regulated SUMO interaction modules connect the SUMO system to CK2 signaling. *Mol. Cell.* 33:400–409. http://dx.doi.org/10.1016/j.molcel.2009.01.013

Tabor, S., and C.C. Richardson. 1985. A bacteriophage T7 RNA polymerase/promoter system for controlled exclusive expression of specific genes. *Proc. Natl. Acad. Sci. USA.* 82:1074–1078. http://dx.doi.org/10.1073/pnas.82.4.1074

Tanaka, K., J. Nishide, K. Okazaki, H. Kato, O. Niwa, T. Nakagawa, H. Matsuda, M. Kawamukai, and Y. Murakami. 1999. Characterization of a fission yeast SUMO-1 homologue, pmt3p, required for multiple nuclear events, including the control of telomere length and chromosome segregation. *Mol. Cell. Biol.* 19:8660–8672. http://dx.doi.org/10.1128/MCB.19.12.8660

Wang, F., J. Dai, J.R. Daum, E. Niedzialkowska, B. Banerjee, P.T. Stukenberg, G.J. Gorbsky, and J.M. Higgins. 2010. Histone H3 Thr-3 phosphorylation by haspin positions Aurora B at centromeres in mitosis. *Science.* 330:231–235. http://dx.doi.org/10.1126/science.1189435

Wang, F., N.P. Ulyanova, M.S. van der Waal, D. Patnaik, S.M. Lens, and J.M. Higgins. 2011. A positive feedback loop involving haspin and Aurora B promotes CPC accumulation at centromeres in mitosis. *Curr. Biol.* 21:1061–1069. http://dx.doi.org/10.1016/j.cub.2011.05.016

Welburn, J.P., M. Vleugel, D. Liu, J.R. Yates III, M.A. Lampson, T. Fukagawa, and I.M. Cheeseman. 2010. Aurora B phosphorylates spatially distinct targets to differentially regulate the kinetochore-microtubule interface. *Mol. Cell.* 38:383–392. http://dx.doi.org/10.1016/j.molcel.2010.02.034

Xue, Y., F. Zhou, C. Fu, Y. Xu, and X. Yao. 2006. SUMOsp: A web server for sumoylation site prediction. *Nucleic Acids Res.* 34(Web Server):W254-7. http://dx.doi.org/10.1093/nar/gkl207

Yamagishi, Y., T. Honda, Y. Tanno, and Y. Watanabe. 2010. Two histone marks establish the inner centromere and chromosome bi-orientation. *Science.* 330:239–243. http://dx.doi.org/10.1126/science.1194498

Zhou, L., X. Tian, C. Zhu, F. Wang, and J.M. Higgins. 2014. Polo-like kinase-1 triggers histone phosphorylation by haspin in mitosis. *EMBO Rep.* 15:273–281. http://dx.doi.org/10.1002/embr.201338080